Multi-Area Predictive Control for Combined Electricity and Natural Gas Systems

Michèle Arnold, Rudy R. Negenborn, Göran Andersson, Bart De Schutter

***Abstract*— The optimal operation of an integrated electricity and natural gas system is investigated. The couplings between these two systems are modeled by energy hubs, which serve as interface between the loads and the transmission infrastructures. Previously, we have applied a distributed control scheme to a static three-hub benchmark system. In this paper, we propose an extension of this distributed control scheme for application to energy hubs with dynamics. The dynamics that we consider here are due to storage devices present in the multi-carrier system. We propose a distributed model predictive control approach for improving the operation of the system by taking into account predicted behavior and operational constraints. Simulations in which the proposed scheme is applied to the three-hub benchmark system illustrate the potential of the approach.**

***Index Terms*— Distributed control, model predictive control, electric power systems, natural gas systems, multi-carrier systems**

I. Introduction

Nowadays, infrastructures, such as electricity, natural gas, and local district heating systems, are mostly planned and operated independently of each other. In practice, however, these individual systems are coupled, as e.g., micro combined heat and power plants (μCHP) and other distributed generation plants (such as so-called co- and trigeneration [1]) are used more and more. It is therefore expected that integrated control of several such systems can yield improved performance. The various energy carriers available and the conversion possible between them significantly affect both the technical and the economical operation of energy systems. In particular, consumers get flexibility in supply and could therefore decide in favor of, e.g., cost, reliability, system emissions, availability, or a combination of these.

Currently, research effort is addressing integrated control of combined electricity and natural gas systems [2], [3]. In [3], the couplings between the electricity and gas systems are modeled using the concept of energy hubs [4]. These energy hubs serve as interface between the loads and the transmission infrastructures of both types of systems. The electricity and natural gas system is then modeled as a number of interconnected energy hubs.

Because of the increasing number of distributed generation facilities with mostly fluctuating energy infeed (generation profiles), the issue of storing energy also becomes more important. Electric energy storage devices are expensive and the operation of them causes energy losses. In order to still enable the electric energy supply in time, the operation of a μCHP device in combination with a heat storage device is considered. By optimally using the heat storage device, the μCHP device can be operated in order to follow the electrical load.

In [5], we have proposed a distributed control scheme for the steady-state optimization of energy hub systems. A three-hub benchmark system is used there to illustrate the performance of the approach. In that system, the individual energy hubs determine in a cooperative way which actions to take. The models that the energy hubs thereby use are static, steady-state models. No dynamics are taken into account.

In this paper, we propose an extension of the distributed control scheme presented in [5] for application to energy hubs with dynamics. Here, we in particular consider the dynamics due to storage devices present in the combined electricity and natural gas system. We propose to use a distributed model predictive control (MPC) scheme, in which the operation of the hub system over a certain prediction horizon is considered and in which actions that give the best predicted behavior are determined by the individual energy hubs. By using such a predictive approach, the energy usage can be adapted to expected fluctuations in the energy prices and to expected changes in the load profiles. A variety of distributed MPC approaches have been applied to different application areas, summarized in [6].

This paper is organized as follows. In Section II the mathematical model of the considered multi-carrier system is given. In Section III we first discuss a centralized MPC approach for the overall system and then propose a distributed MPC approach. Simulation results applying the method to a three-hub benchmark system are presented in Section IV. Section V concludes this paper and outlines directions for future research.

II. Modeling

In this section, the model of the combined electricity and natural gas network is presented. The equations for power conversion and power storage within the energy hubs and for power transmission between the hubs are given.

A. System setup

We study general systems consisting of interconnected energy hubs. As example benchmark system we consider a system consisting of three hubs that are interconnected

M. Arnold (corresponding author) and G. Andersson are with the Power Systems Laboratory, ETH Zürich, Physikstrasse 3, 8092 Zürich, Switzerland, e-mail: {arnold,andersson}@eeh.ee.ethz.ch. R.R. Negenborn and B. De Schutter are with the Delft Center for Systems and Control of Delft University of Technology, Mekelweg 2, 2628 CD Delft, The Netherlands, e-mail: r.r.negenborn@tudelft.nl, b.deschutter@dcsc.tudelft.nl. B. De Schutter is also with the Marine and Transport Technology department of Delft University of Technology.

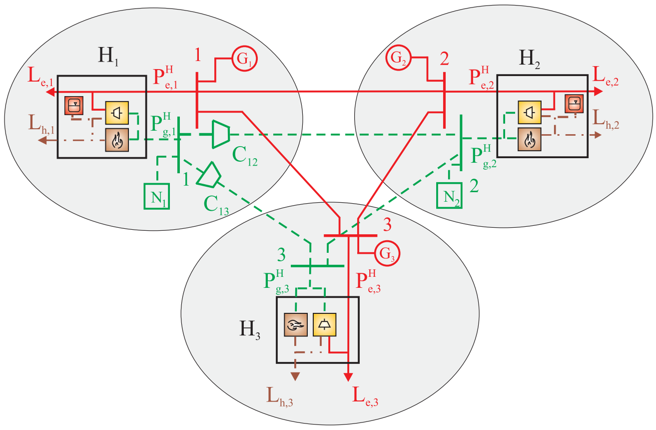

Fig. 1. System setup of three interconnected energy hubs. Active power is provided by generators G_1, G_2, G_3. Hubs H_1 and H_2 have access to adjacent natural gas networks N_1, N_2.

by an electricity and natural gas transmission system, as illustrated in Fig. 1. The electricity system and the gas system are connected via energy hubs. An energy hub is a network node that includes conversion, conditioning, and storage of multiple energy carriers. It represents the interface between the energy sources and transmission lines on the one hand and the power consumers on the other hand. The energy hub is a modeling concept with no restrictions to the size of the modeled system. Single power plants or industrial buildings as well as bounded geographical areas such as whole towns and cities can be modeled as energy hubs.

In the system under study, each energy hub represents a general consumer, e.g., a household, that uses both electricity and gas. Each of the hubs has its own local electrical energy production (G_i, with electric power production $P^{G}_{e,i}$, for $i \in \{1,2,3\}$). Hub H_1 has access to a large gas network N_1, with gas infeed $P^{G}_{g,1}$. In addition, hub H_2 can obtain gas from a smaller local gas tank N_2, modeled as gas infeed $P^{G}_{g,2}$. Each hub consumes electric power $P^{H}_{e,i}$ and gas $P^{H}_{g,i}$, respectively, and supplies energy to its electrical load $L_{e,i}$ and its heat load $L_{h,i}$. The hubs contain converter and storage devices in order to fulfill their energy load requirements. For energy conversion, the hubs contain a μCHP device and a furnace. The μCHP device couples the two energy systems as it simultaneously produces electricity and heat from natural gas. Hubs H_1 and H_2 additionally comprise a hot water storage device. Compressors (C_{ij}, for $(i,j) \in \{(1,2),(1,3)\}$) are present in the gas network within the pipelines originating from hub H_1, at which the large gas network is located. The compressors provide a pressure decay and enable the gas flow to the surrounding gas sinks.

There are several ways in which electrical and thermal load demands can be fulfilled. This redundancy increases the reliability of supply and at the same time provides the possibility for optimizing the input energies, e.g., using criteria such as cost, availability, emissions, etc.

B. Energy hub model

Since we consider an optimization over multiple periods, the equations are defined per time step k. For each of the three energy hubs, the electrical load $L_{e,i}(k)$ and the heat load $L_{h,i}(k)$ at time step k are related to the electricity $P^{H}_{e,i}(k)$ and gas hub input $P^{H}_{g,i}(k)$ as follows:

$$\begin{bmatrix} L_{e,i}(k) \\ L_{h,i}(k) \end{bmatrix} = \begin{bmatrix} 1 & \nu_{g,i}(k)\eta^{CHP}_{g,e,i} \\ 0 & \nu_{g,i}(k)\eta^{CHP}_{g,h,i} + (1-\nu_{g,i}(k))\eta^{F}_{g,h,i} \end{bmatrix} \begin{bmatrix} P^{H}_{e,i}(k) \\ P^{H}_{g,i}(k) \end{bmatrix}, \quad (1)$$

where $\eta^{CHP}_{g,e,i}$ and $\eta^{CHP}_{g,h,i}$ denote the gas-electric and gas-heat efficiencies of the μCHP device (which are assumed to be constant in this paper[1]), and where $\eta^{F}_{g,h,i}$ denotes the efficiency of the furnace. The variable $\nu_{g,i}(k)$ $(0 \leq \nu_{g,i}(k) \leq 1)$ represents a dispatch factor that determines how the gas is divided over the μCHP and the furnace. The term $\nu_{g,i}(k)P^{H}_{g,i}(k)$ defines the gas input power going into the μCHP and the part $(1-\nu_{g,i}(k))P^{H}_{g,i}(k)$ defines the gas input power going into the furnace. As the dispatch factor $\nu_{g,i}(k)$ is variable, different input vectors can be found to fulfill the output loads. This offers additional degrees of freedom in supply.

The storage device is modeled as an ideal storage in combination with a storage interface. In the considered setup, hot water storage devices are implemented. The relation between the heat power exchange $M_{h,i}(k)$ and the effectively stored energy $E_{h,i}(k)$ at a time step k is defined by the following equation:

$$M_{h,i}(k) = \frac{1}{e_{h,i}}\left(E_{h,i}(k) - E_{h,i}(k-1) + E^{stb}_{h,i}\right), \quad (2)$$

where $e_{h,i}$ is the storage efficiency, $E_{h,i}(k)$ denotes the storage energy at the end of period k, and $E^{stb}_{h,i}$ represents the standby energy losses of the heat storage device per period ($E^{stb}_{h,i} \geq 0$). For hubs H_1 and H_2 two hot water storage devices are implemented. Equation (1) is therefore completed with additional storage power flows:

$$\begin{bmatrix} L_{e,i}(k) \\ L_{h,i}(k) + M_{h,i}(k) \end{bmatrix} = \begin{bmatrix} 1 & \nu_{g,i}(k)\eta^{CHP}_{g,e,i} \\ 0 & \nu_{g,i}(k)\eta^{CHP}_{g,h,i} + (1-\nu_{g,i}(k))\eta^{F}_{g,h,i} \end{bmatrix} \begin{bmatrix} P^{H}_{e,i}(k) \\ P^{H}_{g,i}(k) \end{bmatrix}. \quad (3)$$

C. Transmission network

For the transmission networks of both the electricity network and the gas network, power flow models based on nodal power balances are implemented. The power flows for the electricity network are formulated as nodal power balances of the complex power, according to [3], [7]. The power flow equations for the pipeline network are based on nodal volume flow balances. The model of a gas pipeline is composed of a compressor, with pressure amplification p_{inc}, and a pipeline element. More information about the gas network model used can be found in [3].

[1]However, the efficiencies can also be dependent on, e.g., the converted power level.

D. Combined energy hub transmission network model

The combined electricity and gas network is obtained by combining the above stated power flow models. For each time step k an algebraic state vector $\mathbf{z}(k)$ and a dynamic state vector $\mathbf{x}(k)$ are defined. The algebraic state vector includes the variables for which no dynamics are explicitly defined. The dynamic state vector includes variables for which dynamics are included. Hence,

$$\mathbf{x}(k) = \left[\mathbf{E}_{\mathrm{h}}^{\mathrm{T}}(k)\right]^{\mathrm{T}} \tag{4}$$

$$\mathbf{z}(k) = [\mathbf{V}^{\mathrm{T}}(k)\ \boldsymbol{\theta}^{\mathrm{T}}(k)\ \mathbf{p}^{\mathrm{T}}(k)\ \mathbf{p}_{\mathrm{inc}}^{\mathrm{T}}(k)\ (\mathbf{P}_{\mathrm{e}}^{\mathrm{H}})^{\mathrm{T}}(k)\ (\mathbf{P}_{\mathrm{g}}^{\mathrm{H}})^{\mathrm{T}}(k)]^{\mathrm{T}} \tag{5}$$

where

- $\mathbf{V}(k) = [V_1(k), V_2(k), V_3(k)]^{\mathrm{T}}$ and $\boldsymbol{\theta}(k) = [\theta_1(k), \theta_2(k), \theta_3(k)]^{\mathrm{T}}$ denote the voltage magnitudes and angles of the electric buses, respectively,
- $\mathbf{p}(k) = [p_1(k), p_2(k), p_3(k)]^{\mathrm{T}}$ denotes the nodal pressures of all gas buses,
- $\mathbf{p}_{\mathrm{inc}}(k) = [p_{\mathrm{inc},1}(k), p_{\mathrm{inc},2}(k)]^{\mathrm{T}}$ denotes the pressure amplification of the compressors,
- $\mathbf{P}_{\mathrm{e}}^{\mathrm{H}}(k) = [P_{\mathrm{e},1}^{\mathrm{H}}(k), P_{\mathrm{e},2}^{\mathrm{H}}(k), P_{\mathrm{e},3}^{\mathrm{H}}(k)]^{\mathrm{T}}$ denotes the electric inputs of the hubs, and
- $\mathbf{P}_{\mathrm{g}}^{\mathrm{H}}(k) = [P_{\mathrm{g},1}^{\mathrm{H}}(k), P_{\mathrm{g},2}^{\mathrm{H}}(k), P_{\mathrm{g},3}^{\mathrm{H}}(k)]^{\mathrm{T}}$ denotes the gas inputs of the hubs.
- The two storage devices in hub H_1 and H_2 are incorporated in vector $\mathbf{E}_{\mathrm{h}}(k) = [E_{\mathrm{h},1}(k), E_{\mathrm{h},2}(k)]^{\mathrm{T}}$.

At each time step, the control variables $\mathbf{u}(k)$ are defined to include the active power generation of all generators, the natural gas imports of all gas networks and the dispatch factors of each hub, i.e.,

$$\mathbf{u}(k) = \left[(\mathbf{P}_{\mathrm{e}}^{\mathrm{G}})^{\mathrm{T}}(k) \quad (\mathbf{P}_{\mathrm{g}}^{\mathrm{G}})^{\mathrm{T}}(k) \quad \boldsymbol{\nu}_{\mathrm{g}}^{\mathrm{T}}(k)\right]^{\mathrm{T}}, \tag{6}$$

where

- $\mathbf{P}_{\mathrm{e}}^{\mathrm{G}}(k) = [P_{\mathrm{e},1}^{\mathrm{G}}(k), P_{\mathrm{e},2}^{\mathrm{G}}(k), P_{\mathrm{e},3}^{\mathrm{G}}(k)]^{\mathrm{T}}$ denotes the active power generation of all generators,
- $\mathbf{P}_{\mathrm{g}}^{\mathrm{G}}(k) = [P_{\mathrm{g},1}^{\mathrm{G}}(k), P_{\mathrm{g},2}^{\mathrm{G}}(k)]^{\mathrm{T}}$ defines the natural gas imports and
- $\boldsymbol{\nu}_{\mathrm{g}}(k) = [\nu_{\mathrm{g},1}(k), \nu_{\mathrm{g},2}(k), \nu_{\mathrm{g},3}(k)]^{\mathrm{T}}$ describes the dispatch factors of the gas input junctions.

Now, the model that we use to represent the combined electricity and gas network can be conveniently written as

$$\mathbf{x}(k+1) = \mathbf{f}(\mathbf{x}(k), \mathbf{z}(k), \mathbf{u}(k)) \tag{7}$$

$$\mathbf{0} = \mathbf{g}(\mathbf{x}(k), \mathbf{z}(k), \mathbf{u}(k)), \tag{8}$$

summarizing the power flow equations of the electricity and gas system, and the hub equations.

III. Control Problem Formulation

In this section we discuss the control of the system introduced above. We first discuss how MPC can be used in the form of a centralized, supervisory controller that can measure all variables in the network and that determines actions for all actuators. Due to practical and computational issues implementing such a centralized controller may not be feasible. Individual hubs may not want to give access to their sensors and actuators to a centralized authority and even if they would allow a centralized authority to take over control of their hubs, this centralized authority could have computational problems with respect to required time when solving the resulting centralized control problem. We therefore also discuss a distributed MPC scheme, in which the control is spread over the individual hubs.

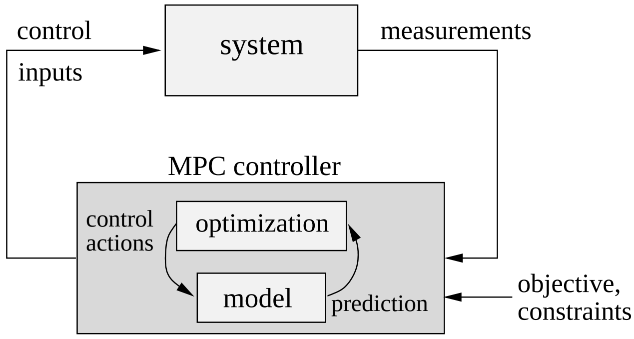

Fig. 2. Illustration of model predictive control.

The goal of either control scheme is to determine values for the control variables $\mathbf{u}(k)$ in such a way that the costs for electricity generation and natural gas usage are minimized. Hence, the control problem can be stated as determining the inputs $\mathbf{u}(k)$ in such a way that the control objectives are achieved, while satisfying the system constraints.

As control strategy we propose to use MPC. MPC [8], [9] is a control strategy that uses an internal model for making predictions of the system behavior over a predefined prediction horizon with length N, thereby also taking into account operational constraints. MPC is suited for control of multi-carrier systems, since it can adequately take into account the dynamics of energy storage devices and the characteristics of the electricity and gas networks. MPC operates in a receding horizon fashion, meaning that at each time step new measurements of the system and new predictions into the future are made. By using MPC, actions can be determined that anticipate future events, such as increasing or decreasing energy prices.

In Fig. 2 MPC is illustrated schematically. At each control step k, an MPC controller first measures the current state of the system, $\mathbf{x}(k)$. Then, it determines using (numerical) optimization which control input $\mathbf{u}(k)$ to provide by finding the actions that over a prediction horizon of N time steps give the best predicted performance according to a given objective function. The control variables determined for the first prediction step are applied to the system. The system then transitions to a new state, $\mathbf{x}(k+1)$, after which the cycle starts all over.

A. Centralized model predictive control

In the centralized MPC formulation there is a single controller that determines the inputs $\mathbf{u}(k)$ for the whole network. The control objective[2] is to minimize the energy

[2] In addition to the stated objectives, it would be straightforward to also include voltage regulation and power flow limitations as control objectives.

costs, represented by the following system-wide objective function:

$$J = \sum_{l=0}^{N-1} \sum_{i \in G} q_i^{\mathrm{G}}(k+l)(P_{\mathrm{e},i}^{\mathrm{G}}(k+l))^2 + q_i^{\mathrm{N}}(k+l)(P_{\mathrm{g},i}^{\mathrm{G}}(k+l))^2, \quad (9)$$

where G includes all generation units, i.e., the tree generators and the two natural gas imports. The prices for electricity generation $q_i^{\mathrm{G}}(k)$ and for natural gas consumption $q_i^{\mathrm{N}}(k)$ can vary throughout the day. The centralized control problem formulation is now stated as

$$\min_{\tilde{\mathbf{u}}(k)} J(\tilde{\mathbf{x}}(k+1), \tilde{\mathbf{z}}(k), \tilde{\mathbf{u}}(k)) \quad (10)$$

subject to

$$\tilde{\mathbf{x}}(k+1) = \tilde{\mathbf{f}}(\tilde{\mathbf{x}}(k), \tilde{\mathbf{z}}(k), \tilde{\mathbf{u}}(k)) \quad (11)$$

$$\tilde{\mathbf{g}}(\tilde{\mathbf{x}}(k), \tilde{\mathbf{z}}(k), \tilde{\mathbf{u}}(k)) = \mathbf{0} \quad (12)$$

$$\tilde{\mathbf{h}}(\tilde{\mathbf{x}}(k), \tilde{\mathbf{z}}(k), \tilde{\mathbf{u}}(k)) \leq \mathbf{0}, \quad (13)$$

where the tilde over a variable represents that variable over a prediction horizon of N steps, e.g., $\tilde{\mathbf{u}}(k) = [\ \mathbf{u}(k)^{\mathrm{T}}, \ldots, \mathbf{u}(k+N-1)^{\mathrm{T}}\ ]^{\mathrm{T}}$. The inequality constraints (13) comprise limits on the voltage magnitudes, active and reactive power flows, pressures, changes in compressor settings, and dispatch factors. Furthermore, power limitations on the hub inputs and on gas and electricity generation are also incorporated in (13). Regarding the storage devices, limits on the storage contents and the storage flows are imposed.

The optimization problem (10)–(13) is a nonlinear programming problem [10], which can be solved using optimization problem solvers for nonlinear programming, such as sequential quadratic programming [10]. In general, the solution space is non-convex and therefore finding the global optimum cannot be guaranteed with numerical methods.

B. Distributed model predictive control

In the distributed MPC formulation, there is no single controller, but there are multiple controllers which act in a cooperative way. Each controller is responsible for its own part of the overall system. In our case there are three individual controllers each of which controls a particular area. In addition, the compressors in the gas networks are controlled by the controller of energy hub H_1.

In the distributed MPC formulation each individual controller has its own control objective. In particular, the objective functions of the three controllers are:

$$J_1 = \sum_{l=0}^{N-1} q_1^{\mathrm{G}}(k+l)(P_{\mathrm{e},1}^{\mathrm{G}}(k+l))^2 + q_1^{\mathrm{N}}(k+l)(P_{\mathrm{g},1}^{\mathrm{G}}(k+l))^2 \quad (14a)$$

$$J_2 = \sum_{l=0}^{N-1} q_2^{\mathrm{G}}(k+l)(P_{\mathrm{e},2}^{\mathrm{G}}(k+l))^2 + q_2^{\mathrm{N}}(k+l)(P_{\mathrm{g},2}^{\mathrm{G}}(k+l))^2 \quad (14b)$$

$$J_3 = \sum_{l=0}^{N-1} q_3^{\mathrm{G}}(k+l)(P_{\mathrm{e},3}^{\mathrm{G}}(k+l))^2. \quad (14c)$$

Each control agent is responsible for the hub variables and all system variables of the nodes connected to it. For the first controller, the state and control vectors for each time step k are defined as

$$\mathbf{x}_1(k) = [\mathrm{E}_1(k)]^{\mathrm{T}} \quad (15)$$

$$\mathbf{z}_1(k) = [V_1(k), \theta_1(k), p_1(k), p_{\mathrm{inc},1}(k), p_{\mathrm{inc},2}(k), P_{\mathrm{e},1}^{\mathrm{H}}(k), P_{\mathrm{g},1}^{\mathrm{H}}(k)]^{\mathrm{T}} \quad (16)$$

$$\mathbf{u}_1(k) = [P_{\mathrm{e},1}^{\mathrm{G}}(k), P_{\mathrm{g},1}^{\mathrm{G}}(k), \nu_{\mathrm{g},1}(k)]^{\mathrm{T}} \quad (17)$$

The state and control vectors for the second and third controller are defined similarly according to Fig. 1 (grey areas).

Each controller solves its own local MPC problem using the local model of its hub. However, this local MPC problem depends on the MPC problems of the other controllers, since the electricity and gas networks interconnect the hubs. Therefore, the MPC optimization problems of the controllers have to be solved in a cooperative way. This is not only to ensure that the controllers choose feasible actions, but also to allow the controllers to choose actions that are optimal from a system-wide point of view. The distributed MPC approach that we propose in this paper is based on using the Lagrangian relaxation procedure derived in [11] for setting up the MPC optimization problems of the individual controllers and for determining which information has to be exchanged among the controllers.

We next illustrate the mathematical procedure to decompose a general centralized MPC optimization problem of a centralized controller into optimization problems for individual distributed controllers. The procedure is illustrated on a system consisting of two interconnected areas, extension to three or more areas is straightforward.

Consider two areas A and B which comprise the system variables $\tilde{\mathbf{y}}_{\mathrm{A}}(k)$ and $\tilde{\mathbf{y}}_{\mathrm{B}}(k)$, respectively. For demonstration purposes, we collect all variables introduced above in a vector $\tilde{\mathbf{y}}(k)$, e.g., $\tilde{\mathbf{y}}_{\mathrm{A}}(k) = [\tilde{\mathbf{x}}_{\mathrm{A}}(k), \tilde{\mathbf{z}}_{\mathrm{A}}(k), \tilde{\mathbf{u}}_{\mathrm{A}}(k)]^T$. The centralized MPC optimization problem is then specified as

$$\min_{\tilde{\mathbf{u}}_{\mathrm{A}}(k),\ \tilde{\mathbf{u}}_{\mathrm{B}}(k)} J(\tilde{\mathbf{y}}_{\mathrm{A}}(k), \tilde{\mathbf{y}}_{\mathrm{B}}(k)) \quad (18)$$

$$\text{subject to} \quad \tilde{\mathbf{g}}(\tilde{\mathbf{y}}_{\mathrm{A}}(k), \tilde{\mathbf{y}}_{\mathrm{B}}(k)) = \mathbf{0}. \quad (19)$$

Here, only equality constraints are explained for demonstration purposes. Inequality constraints are handled analogously.

For decomposing the centralized MPC optimization problem, both the objective and the equality constraints are separated and assigned to a responsible control agent (Fig. 3). Both areas comprise constraints involving only the own system variables, $\tilde{\mathbf{g}}_{\mathrm{A}}(\tilde{\mathbf{y}}_{\mathrm{A}}(k))$, $\tilde{\mathbf{g}}_{\mathrm{B}}(\tilde{\mathbf{y}}_{\mathrm{B}}(k))$. Besides them, so-called *coupling constraints* are introduced, containing variables from both areas (marked by a hat). Regarding the objectives, both objective functions consist of two parts. The first term expresses the main objective originating from the overall objective function (18). The second term is responsible for the coordination between the agents and consists of the coupling constraints introduced above. As indicated in Fig. 3, the coupling constraints are kept explicitly as hard constraints in the constraint set of one control agent

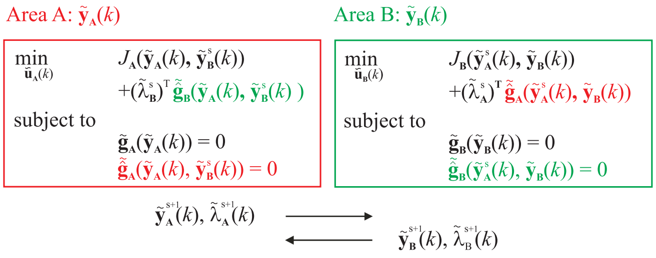

Fig. 3. Decomposition procedure applied to a two-area system (area A: $\tilde{\mathbf{y}}_A(k)$, area B: $\tilde{\mathbf{y}}_B(k)$) and variables to be exchanged after each iteration counter s.

and added as soft constraints to the main objective of the other control agent (modified Lagrangian relaxation procedure [11]). The weighting factors of the soft constraints are the Lagrangian multipliers obtained from the optimization problem of the other area. Both the objectives and the coupling constraints depend on variables of the other area, indicated by the superscript s. To handle this dependency, the optimization problems of the control agents are solved in an iterative procedure. At each iteration step s, the MPC optimization problems of both control agents are solved independently of each other, while keeping the variables of the neighboring area constant. After each iteration, the control agents exchange the updated values of their variables as indicated in Fig. 3, i.e., the variables $\tilde{\mathbf{y}}_i^{s+1}(k)$ and the Lagrangian multipliers $\tilde{\boldsymbol{\lambda}}_i^{s+1}(k)$. Convergence is achieved when the exchanged variables do not change more than a small tolerance γ_{tol} in two consecutive iterations. In contrary to conventional Lagrangian relaxation procedures, a faster convergence is achieved as the weighting factors are represented by the Lagrangian multipliers of the neighboring optimization problems [11].

Applying this procedure to combined electricity and gas systems, the electric power flow and gas flow equations at the peripheral buses serve as coupling constraints. For the studied three-hub system, the active power balances of all nodes of the electricity system enforce a coordination as they depend on the neighboring voltage magnitudes and angles. Regarding the gas system, the nodal flow balances of all buses depend on the pressures of the neighboring buses and therefore enforce a coordination as well. Summarizing, for each area, there exists one coupling constraint for the electricity and one for the natural gas system, specified in [3].

IV. Case Study

In this section a case study is presented in which the proposed distributed MPC scheme is applied to the illustrative three-hub system. However, the scheme is general and not only valid or applicable for the system depicted in Fig. 1. The performance of the distributed approach is compared with the performance of the centralized MPC approach. The solver `fmincon` provided by the Optimization Toolbox of Matlab is used [12].

A. Simulation setup

Each hub has a daily profile of its load demand and also of the energy prices. In this preliminary case study, a perfect forecast is assumed, in which no disturbances within the known profiles are occurring. The generation costs are minimized for a simulation horizon $N_{\text{sim}} = 10$. The length of the prediction horizon N is chosen as $N = 3$. Hence, an optimization over N time steps is run N_{sim} times, at each time step k implementing only the control variable for the current time step k and then starting a new optimization at time step $k+1$ with updated system measurements.

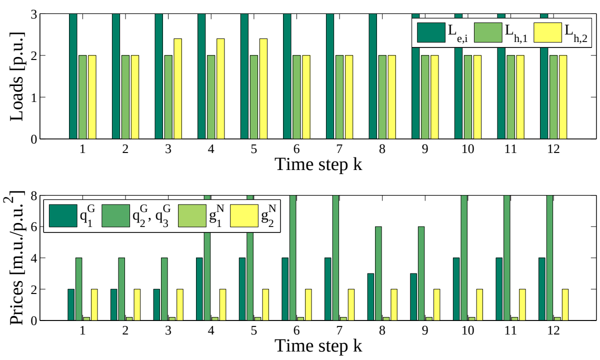

Fig. 4. Profile for electricity $L_{e,i}(k)$ and heat loads $L_{h,i}(k)$ (upper plot) and prices for electricity $q_i^G(k)$ and natural gas consumption $q_i^N(k)$ (lower plot).

Given are the price and load profiles of all hubs (Fig. 4). The electricity load $L_{e,i}$ and the gas import prices q_i^N remain constant over time. Variations are assumed only in the prices of the electric energy generation units $q_i^G(k)$ and in the heat load of hub H_2, $L_{h,2}$, in order to exactly retrace the storage behavior. Further details about the coefficients and simulation parameters used can be found in [3].

B. Single simulation step

In order to evaluate whether the solution determined by the distributed algorithm is feasible for the real system, the following simulation is run. In Fig. 5 the quality of the intermediate solutions in case that these would be applied to the system is shown. The distributed MPC optimization problem is is solved at time step $k = 1$, for $N = 3$. At each iteration counter s, the overall system costs are shown, when applying the control variables determined by the distributed algorithm to the system. The dotted values refer to the infeasible solutions. As the number of iterations increases, the distributed MPC converges, and, in fact, the solution obtained at the end of the iterations approaches the solution obtained by the centralized MPC approach (200.98 p.u.). After iteration 16, the values of all control variables are feasible. After 39 iterations, the algorithm converges.

C. Simulation of multiple time steps

When minimizing the energy costs over the full simulation of N_{sim} time steps, a total cost of 850.62 p.u. is obtained for the above given load and price profiles. Applying centralized MPC, the overall costs are lower, 849.78 p.u., since, due to the imposed convergence tolerance γ_{tol} of the distributed algorithm, the centralized approach finds a slightly different solution at some iteration steps. In Fig. 6, the active power

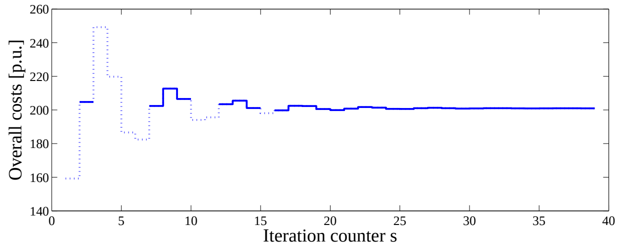

Fig. 5. Intermediate solutions of the distributed algorithm applied to the system. Dotted lines represent infeasible solutions, solid lines are feasible solutions.

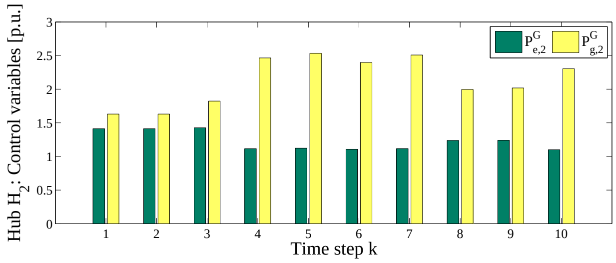

Fig. 6. Active power generation $P^{G}_{e,2}$ and natural gas import $P^{G}_{g,2}$ of hub H_2 over time.

generation and the natural gas import of hub H_2 are shown. As can be seen, active power generation is reduced at time steps with higher generation costs, i.e., time steps 4–7 and time step 10. During these time steps more gas is consumed. The electrical loads are now predominantly supplied by the μCHP devices in order to save costs. Most of the gas is diverted into the μCHP device and less into the furnace. For still supplying the heat load, the heat storage devices come into operation. Figure 7 shows the content of both storage devices evolving over the time steps. Both storage devices start at an initial level of 1.5 p.u. Since the heat load at hub H_2 is increased by 20% at time steps 3-5 (Fig. 4), storage E_2 attempts to remain full before this increase and then operates at its lower limit during the heat load peaks. At the proceeding electricity price peaks (time steps 6, 7) both storages are recharged. The electrical loads are mainly supplied by the μCHP devices and all excessive heat produced during these time steps is then stored in the storage devices. Storage device E_1 is refilled more than E_2, as hub H_2 has a limited gas access.

If the controllers have a shorter prediction horizon than $N = 3$, the storage devices are filled up less and also later. With a prediction horizon length of $N = N_{\text{sim}}$, the storage devices are filled up earlier and the lowest costs are obtained, although calculation time becomes considerably longer and the system is insensitive to unknown changes in the load and price profiles.

V. Conclusions and Future Research

In this paper we have proposed a distributed model predictive control (MPC) approach for control of energy hub systems. A distributed MPC scheme is proposed, such that dynamics due to, e.g., storage devices, forecasts on energy prices and demand profiles, and operational constraints can

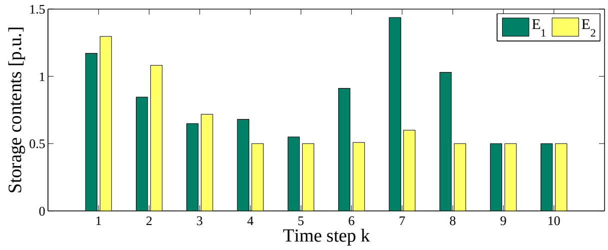

Fig. 7. Evolution of storage contents (E_1, E_2) over time.

be taken into account adequately. We have applied this approach for minimizing generation costs of a particular three-hub integrated electricity and natural gas system. In a case study, we have analyzed the quality of intermediate solutions obtained throughout the iterations of the proposed approach to ensure that applying the control to the real system yields feasible solutions. In future research the performance under different control horizons will be compared. Furthermore, conditions and measures for guaranteeing convergence have to be investigated more precisely. In addition, we will address the incorporation of disturbances in the scheme instead of assuming perfect forecasts.

Acknowledgments

This research is supported by the project “Vision of Future Energy Networks” (VoFEN) of ABB, Areva T & D, Siemens, and the Swiss Federal Office of Energy, the European 6th Framework Network of Excellence ”HYbrid CONtrol: Taming Heterogeneity and Complexity of Networked Embedded Systems (HYCON)”, the BSIK project “Next Generation Infrastructures (NGI)”, the Delft Research Center Next Generation Infrastructures, the European STREP project “Hierarchical and distributed model predictive control (HD-MPC)”, and the project “Multi-Agent Control of Large-Scale Hybrid Systems” (DWV.6188) of the Dutch Technology Foundation STW.

References

[1] J. Hernandez-Santoyo and A. Sanchez-Cifuentes, “Trigeneration: An alternative for energy savings,” *Applied Energy*, vol. 76, no. 1–3, pp. 219–277, 2003.

[2] T. W. M. Shahidehpour, Y. Fu, “Impact of natural gas infrastrucutre on electric power systems,” *Proceedings of the IEEE*, vol. 93, no. 5, pp. 1024 – 1056, 2005.

[3] M. Arnold and G. Andersson, “Decomposed electricity and natural gas optimal power flow,” presented at the *16th Power Systems Computation Conference (PSCC 08)*, Glasgow, Scotland, 2008.

[4] M. Geidl and G. Andersson, “Optimal power flow of multiple energy carriers,” *IEEE Transactions on Power Systems*, vol. 22, no. 1, pp. 145–155, 2007.

[5] M. Arnold, R. R. Negenborn, G. Andersson, and B. De Schutter, “Distributed control applied to combined electricity and natural gas infrastructures,” in *Proceedings of the International Conference on Infrastructure Systems*, Rotterdam, The Netherlands, Nov. 2008.

[6] R. Scattolini, “Architectures for distributed and hierarchical model predictive control - a review,” *Journal of Process Control*, vol. 19, no. 5, pp. 723–731, 2009.

[7] P. Kundur, *Power System Stability and Control*. New York, New York: McGraw-Hill, 1994.

[8] J. M. Maciejowski, *Predictive Control with Constraints*. Harlow, England: Prentice Hall, 2002.

[9] E. F. Camacho and C. Bordons, *Model Predictive Control*. New York, New York: Springer-Verlag, 2004.

[10] D. P. Bertsekas, *Nonlinear Programming*. Beltmore, Massachusetts: Athena Scientific, 2003.

[11] F. J. Nogales, F. J. Prieto, and A. J. Conejo, “A decomposition methodology applied to the multi-area optimal power flow problem,” *Annals of Operations Research*, vol. 120, pp. 99–116, Apr. 2003.

[12] The Mathworks, “Optimization Toolbox User’s Guide,” 2008. [Online]. Available: http://www.mathworks.com/